CHEMISTRY
A EUROPEAN JOURNAL

DOI: 10.1002/chem.200501569

Ab Initio Molecular Dynamics Studies of Ionic Dissolution and Precipitation of Sodium Chloride and Silver Chloride in Water Clusters, $NaCl(H_2O)_n$ and $AgCl(H_2O)_n$, $n = 6$, 10, and 14

Chi-Kit Siu,*[a, b] Brigitte S. Fox-Beyer,[a] Martin K. Beyer,*[a, c] and Vladimir E. Bondybey*[a]

Abstract: An ab initio molecular dynamics method was used to compare the ionic dissolution of soluble sodium chloride (NaCl) in water clusters with the highly insoluble silver chloride (AgCl). The investigations focused on the solvation structures, dynamics, and energetics of the contact ion pair (CIP) and of the solvent-separated ion pair (SSIP) in $NaCl(H_2O)_n$ and $AgCl(H_2O)_n$ with cluster sizes of $n = 6$, 10 and 14. We found that the minimum cluster size required to stabilize the SSIP configuration in $NaCl(H_2O)_n$ is temperature-dependent. For $n = 6$, both configurations are present as two distinct local minima on the free-energy profile at 100 K, whereas SSIP is unstable at 300 K. Both configurations, separated by a low barrier ($< 10\ kJ\,mol^{-1}$), are identifiable on the free energy profiles of $NaCl(H_2O)_n$ for $n = 10$ and 14 at 300 K, with the Na^+/Cl^- pairs being internally solvated in the water cluster and the SSIP configuration being slightly higher in energy ($< 5\ kJ\,mol^{-1}$). In agreement with the low bulk solubility of AgCl, no SSIP minimum is observed on the free-energy profiles of finite $AgCl(H_2O)_n$ clusters. The AgCl interaction is more covalent in nature, and is less affected by the water solvent. Unlike NaCl, AgCl is mainly solvated on the surface in finite water clusters, and ionic dissolution requires a significant reorganization of the solvent structure.

Keywords: ab initio calculations · hydrogen bonds · ionic dissolution · molecular dynamics · water clusters

Introduction

Dissolution and precipitation of salts are fundamental processes in solution chemistry. Dissolved salts, such as sodium chloride (NaCl), play important roles in both inorganic and organic reactions,[1,2] and particularly in biochemistry, for instance, biological growth[3–6] and solubility of biomolecules in salt buffers.[7] They are also important in marine chemistry[8] and for the formation and reactivity of aerosols in the atmosphere.[9–12] The dissolution and precipitation of salts in aqueous systems are widely used in our daily life, for example, in wastewater treatment by precipitation,[13] wound healing,[14] and prevention of hailstorms by providing nucleation seeds in clouds to stimulate rain.[15] One of the most classic reactions in analytical chemistry is the precipitation of halide ions with silver nitrate. Therefore, the solvation of salts has been extensively investigated experimentally,[16–27] as well as theoretically.[28–40]

Recent experiments have shown that ionized substances are present not only in bulk solutions, but also in small, finite clusters.[41–45] Clearly, the stabilization energy of an ion depends on the number of solvent molecules in its solvation shell, and this raises the question what minimum amount of solvent is required to stabilize the ionized substances.[46–48] Our experiments, employing Fourier transform ion cyclotron

[a] Dr. C.-K. Siu, Dr. B. S. Fox-Beyer, Priv.-Doz. Dr. M. K. Beyer, Prof. Dr. V. E. Bondybey
Department Chemie, Physikalische Chemie 2
Technische Universität München
Lichtenbergstrasse 4, 85747 Garching (Germany)
Fax: (+49) 89-289-13416
E-mail: cksiu@yorku.ca
martin.beyer@mail.chem.tu-berlin.de
bondybey@gmail.com

[b] Dr. C.-K. Siu
Present address:
Department of Chemistry and Centre for Research in Mass Spectrometry, York University
4700 Keele Street, Toronto, Ontario M3J 1P3 (Canada)

[c] Priv.-Doz. Dr. M. K. Beyer
Present address:
Institut für Chemie, Sekr. C4, Technische Universität Berlin
Strasse des 17. Juni 135, 10623 Berlin (Germany)

Supporting information for this article is available on the WWW under http://www.chemeurj.org/ or from the author: Cartesian coordinates and calculated energies for the structures shown in Figure 1, optimized at different level of theory. Movies, in mpeg format, for selected simulation trajectories (Figures 3 and 6 with a cluster size of $n = 14$). Table S1: Results of the benchmark calculations of 1:1 ion–water complexes. Table S2: Results of calculations of $NaCl(H_2O)_6$ at different levels of theory. Figures S1 and S2: Orientation of water molecules in the first solvation shell of solvated ions.

resonance (FT-ICR) mass spectrometry, have demonstrated that acids, such as HCl, or highly soluble salts, such as NaCl, will ionically dissolve in ionic clusters of the type $H^+(H_2O)_n$ when $n>11$.[45,49,50] It is interesting to compare this number with the bulk solubility product $K_{sp} = 37.9\,mol^2L^{-2}$ of sodium chloride (at 25 °C),[51] which gives a solute/solvent molecular ratio of approximately 1:9. More recently, Castleman and co-workers have used femtosecond pump-probe spectroscopy to show that dissolution of HBr in water clusters to form $H^+(H_2O)_nBr^-$ occurs with a minimum size of $n = 5$.[47] Ionic dissolution in small water clusters provides invaluable insights into the solvation chemistry at the interface between droplets of airborne moisture and particles of sea salt where molecular halogens are generated that contribute to ozone formation and depletion in the troposphere.[10–12]

Establishing this minimum number of solvent molecules is of course important for a detailed, microscopic understanding of the solvation process, and the availability of experimental data on ionic dissolution in clusters has motivated a number of theoretical investigations.[52–58] The addition of water molecules to a diatomic polar species, such as NaCl, favors charge separation and also increases the polarity of such a contact ion pair (CIP).[54,57] When the number of solvent molecules increases, the ions can separate with the water molecules penetrating the area between them to result in a solvent-separated ion pair (SSIP).[53,56] On the basis of his ab initio studies of NaCl, Jungwirth has come to the conclusion that six water molecules are sufficient to form such a SSIP.[56]

Unlike ionic sodium chloride (NaCl), the bond in silver chloride (AgCl) is more covalent in character and significantly stronger. In fact, AgCl in bulk water is one of the most insoluble salts, with a solubility product of only $K_{sp} = 1.77\times10^{-10}\,mol^2L^{-2}$ (at 25 °C),[51] which is why precipitation with silver nitrate is frequently used for the quantitative determination of halide ions in aqueous solution. Recent FT-ICR mass spectrometric studies have revealed that AgCl, similar to other transition metals in oxidation state I, behaves quite differently compared to soluble salts in ionic water clusters.[45,59] When an Ag^+ cation and a Cl^- anion are both introduced into a cluster, they seem to immediately "precipitate" from the solution to form a covalent AgCl molecule, or, in other words, an AgCl CIP. Very recent theoretical studies of small water clusters have also shown that the AgCl CIP is more stable than the AgCl SSIP.[60] $AgCl(H_2O)_n$ aerosols are formed by volcanic activity, and understanding their solvation properties is important for atmospheric chemistry.[61]

Even though recent calculations show that the NaCl SSIP represents a local minimum on the potential energy surface of a cluster with six water molecules,[56] it may not be stable when thermal and entropic effects are considered.[36,39] Intuitively, molecules such as HCl are more soluble at a higher temperature, as evidenced by its ionic dissociation on a HCl-covered film of ice.[62,63] One might expect differences between HCl and NaCl because the $H^+\cdots H_2O$ interaction is much stronger than the $Na^+\cdots H_2O$ interaction. Such temperature effects are not only crucial when comparing calculations with laboratory experiments, but they are also critical to the understanding of chemical reactions in the atmosphere. Although ab initio calculations do yield the static geometry of a cluster, they do not give a clear picture of the thermal molecular motions. The ab initio molecular dynamics (AIMD) method has been widely used to study the dynamics of the solvation process of ions, both in the gas phase and in condensed phases.[64–66] In the present work, we use an AIMD method based on density functional theory (DFT) to gain insights into thermal effects upon ion solvation. We investigate the temperature effects on the stability of the CIP and SSIP of $NaCl(H_2O)_n$ clusters, the free-energy profiles of the ionic dissolution of NaCl and AgCl in water clusters, $NaCl(H_2O)_n$ and $AgCl(H_2O)_n$, with cluster sizes of $n = 6$, 10 and 14 at a temperature of 300 K, and their structural changes along the solvation reaction coordinate.

Computational Methods

The present ab initio molecular dynamics (AIMD) studies of NaCl and AgCl hydration were carried out using the Vienna Ab Initio Simulation Package (VASP),[67–70] which is based on density functional theory (DFT) with planewave basis sets. Local density approximation (LDA) with Perdew–Wang gradient correction (PW91)[71] was used for the exchange-correlation functional that employ closed-shell electronic structure calculations for the ionic dissolution in the water clusters. We used directly the optimized pseudopotentials for the H, O, Cl, Na, and Ag atoms supplied with the VASP program,[72] which were constructed by means of the projector augmented wave (PAW) method with the valence wavefunctions containing all nodes in the core region.[73] In order to minimize the interaction between the periodical images imposed by the planewave basis set, the water clusters were located in a cubic box with a large lattice parameter (15 Å for $n = 6$ and 10, and 16 Å for $n = 14$). A planewave basis set with a cutoff energy (E_{cutoff}) of 262 eV was used for the electronic wavefunctions, which were computed by RMM-DIIS minimization for the total electronic energy.

The structures and energies of 1:1 ion–water complexes calculated by VASP are in good agreement with those calculated for other levels of theory using the Gaussian 98 quantum chemistry program[74] as well as experimental data.[75–77] A summary of these benchmark calculations is provided as Table S1 in the Supporting Information. The use of a planewave basis set with a finite cutoff energy (E_{cutoff}) may introduce computational errors; however, the hydration energies ΔE for all complexes predicted by VASP with $E_{cutoff} = 262$ eV (set I) are consistently higher by only $\approx 12\,kJ\,mol^{-1}$ compared to those calculated with the Gaussian 98 program. Increasing the cutoff energy to $E_{cutoff} = 400$ eV (set II in Table S1) slightly improves the ΔE values, but raises the computational costs considerably. Nevertheless, the opti-

mized structures obtained from VASP with both set I and set II are in good agreement with those from other levels of theory. It is worth noting that enthalpic and entropic contributions are significant for ion–water clusters with fluxional structures ($T\Delta S \approx 30\,\mathrm{kJ\,mol^{-1}}$, included in the ΔG values listed in Table S1). The effects are even more important for larger clusters, which will be discussed below, and may change the relative stability of different isomers. This illustrates that high-level ab initio calculations, while superior in their description of the equilibrium geometry, do not provide sufficient information about the behavior of the clusters at elevated temperatures. AIMD simulations provide essential information on the dynamics of the system.

AIMD simulations were performed on the Born–Oppenheimer potential surface described by the DFT electronic structure, solving the equations of motion with integration timesteps of 0.5 femtoseconds (fs). For each AIMD run, the dynamics were simulated for at least 4 picoseconds (ps), which amounts to 8000 timesteps, in order to reduce the fluctuation in the average total potential energy to less than 0.1 %, which roughly equals $5\,\mathrm{kJ\,mol^{-1}}$ or $2kT$ at $T = 300$ K. The temperature of the cluster was controlled by a Nosé–Hoover thermostat.[78] The thermodynamics and mechanism of the ionic dissolution of Na–Cl and Ag–Cl in water clusters were studied by distance-constrained molecular dynamics employing the RATTLE algorithm,[79] with the Na···Cl and Ag···Cl distances treated as the reaction coordinates.

Results and Discussion

Temperature effects in the ionic dissolution of NaCl in $NaCl(H_2O)_6$: During the course of the ionic dissolution of a NaCl molecule in water one can define two important intermediate states (contact ion pair (CIP) and solvent separated ion pair (SSIP)) that depend on the distance between the two component ions. Recent ab initio calculations suggest that the interionic distance between Na^+ and Cl^- in the CIP and the SSIP structures of $NaCl(H_2O)_6$ differ by nearly 2 Å.[56] In this section, we investigate the CIP and the SSIP structures of $NaCl(H_2O)_6$ further, both with the help of the Gaussian 98 program employing various levels of theory and different basis sets, and with the VASP dynamics simulation package that takes account of thermal effects.

In the Gaussian 98 studies, we constrained the CIP geometry to C_3 symmetry and the SSIP geometry to C_{3v} symmetry in order to reduce the computational costs. Our computations on the $NaCl(H_2O)_6$ clusters confirm both the CIP and the SSIP configurations to be local minima on the overall potential surface, whose geometries are shown in Figure 1, and whose energies relative to the energy of the most stable

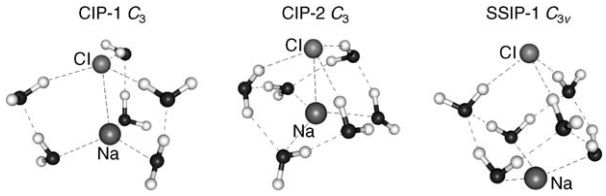

Figure 1. Optimized geometries for the $NaCl(H_2O)_6$ cluster, whose energies versus the most stable CIP-1 isomer are listed in Table 1. The contact ion pair CIP-2 and the solvent-separated ion pair SSIP are similar to the structures studied by Jungwirth.[56] The CIP-1, global minimum according to the present study at both MP2 and BPW91 levels, can be obtained at the BPW91/BS2 or BS3 levels by geometry relaxation of CIP-2.

CIP-1 isomer are listed in Table 1. The isomer with a larger positive relative energy is less stable compared with the CIP-1 isomer. A complete documentation of all levels of theory used here is provided as Table S2 in the Supporting Information.

In agreement with Jungwirth's results,[56] we found the SSIP structure, which resembles Na^+ and Cl^- ions separated by a cyclic hydrogen-bonded water hexamer. However, we found a configuration, denoted CIP-1, for the contact ion pair that has a lower energy than Jungwirth's CIP structure, shown as CIP-2. In the CIP-2 structure, Na^+ is buried within

Table 1. Energy of isomers relative to that of CIP-1 for $NaCl(H_2O)_6$ calculated with the Gaussian 98 program or VASP. The geometries are shown in Figure 1. (A complete documentation of all theory levels used is shown in Table S2 of Supporting Information).[a]

Level of theory	Basis set		Energy [kJ mol^{-1}]				Na–Cl distance [Å]
			ΔE	$\Delta E_{+\Delta ZPC}$	ΔH (298 K, 1 atm)	ΔG (298 K, 1 atm)	
MP2	BS1	CIP-1	0.0	0.0	0.0	0.0	2.65
		CIP-2	−9.3	−3.6	−7.3	8.6	2.64
		SSIP-1	−5.4	3.4	−2.1	16.1	4.25
	BS2	CIP-1	0.0	0.0	0.0	0.0	2.65
		CIP-2[b]	19.4	20.4	14.1	33.0	2.68
		SSIP-1	−1.5	12.4	4.3	29.6	4.38
BPW91	BS1	CIP-1	0.0	0.0	0.0	0.0	2.78
		CIP-2	3.2	8.0	4.5	18.8	2.82
		SSIP-1	−14.9	−6.3	−12.2	9.0	4.51
	BS3	CIP-1	0.0	0.0	0.0	0.0	2.80
		CIP-2	–	–	–	–	–
		SSIP-1	9.8	18.8	12.5	34.1	4.57
VASP	PW	CIP-1	0.0				2.87
		CIP-2	–				–
		SSIP-1	−2.1				4.58

[a] BS1: H and O: 6-31G**, Cl: 6-31++G**, Na: 6-31G**; BS2: H and O: 6-31++G**, Cl: 6-31++G**, Na: 6-31G**; BS3: H and O: 6-311++G**, Cl: 6-311++G**, Na: 6-311G**; PW = Planewave; $E_{cutoff} = 262$ eV. [b] Two degenerate imaginary frequencies ($-23.2\,\mathrm{cm^{-1}}$).

a cyclic water hexamer, with the chloride anion sticking out towards the cluster periphery. At the MP2/BS1 level (the combination of the basis sets (BS) used for each atom is defined in Table 1), CIP-2 is slightly more stable than the SSIP ($\Delta E_{+\Delta ZPC}$ in Table 1; ZPC: zero-point correction); however, this order reverses on using BS2, including diffuse basis functions on H as well as O atoms. At the BPW91/BS2 or BS3 level, CIP-2 cannot even be located, but it relaxes to another contact ion pair structure CIP-1, the most stable configuration for all levels of theory found in our study. In the CIP-1 structure there is no water hexamer, instead, the structure can be described as a NaCl contact ion pair solvated by three independent water dimers.

The energies of the structures optimized with the VASP program are comparable to the results calculated by the MP2/BS2 method with the Gaussian 98 program (ΔE values in Table 1), the best level of theory in the current studies. The CIP-1 and the SSIP structures are almost isoenergetic in the VASP results. CIP-2 is unstable at the VASP/set II level (Table S2) and cannot even be located at the VASP/set I level. Similar to the 1:1 complex shown in Table 1, the use of a larger cutoff energy for the planewave basis set had no significant effect on both the energies and structures of the cluster isomers investigated (set I and set II listed in Table S2). The smaller cutoff energy (set I with E_{cutoff} = 262 eV) for the planewave basis set is therefore used for all the MD simulations.

In general, CIP-1 is more stable than SSIP when a larger basis set (BS2 or BS3) is used (Table 1). When thermal effects at room temperature ($\Delta H - \Delta E_{ZPC}$) are taken into account, the stability of the SSIP versus the CIP-1 increases, whereby ΔH is always smaller than ΔE_{ZPC}. However, entropic effects ($\Delta G - \Delta H$), however, strongly favor the CIP-1 configuration, where the free energy (ΔG) of the CIP-1 structure is $\approx$30 kJ mol^{-1} lower than that of the SSIP structure at both the MP2 and the BPW91 levels.

The structure of water clusters is highly fluxional owing to the presence of numerous hydrogen bonds. This makes AIMD studies particularly useful because they consider the thermal atomic motions in the water clusters. We first carried out AIMD simulations on $NaCl(H_2O)_6$ at a low temperature of 100 K and starting from either the CIP or the SSIP equilibrium geometry as the initial configuration. The average structures from the AIMD simulations are described by radial distribution functions (RDF), $g_{A-B}(R)$, as shown in Figure 2.

$$N_{A-B} = \int g_{A-B}(R) 4\pi R^2 dR$$

where N_{A-B} is an integration of the correlation-pair A–B with respect to the distance A–B (R). The structures of CIP-1 and SSIP (Figure 1) both remain stable during the 100 K AIMD runs with the C_3 rotational symmetry remaining unchanged. The average structures, described by the RDFs shown in Figure 2, underline this finding. The average Na···Cl distance for the CIP structure (Figure 2a) remains

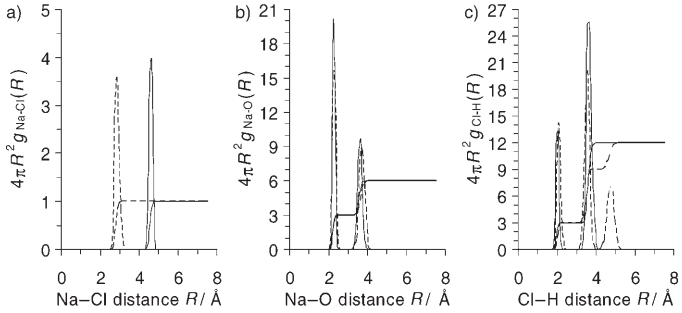

Figure 2. Radial distribution functions (RDF), and curves of their integration, of a) Na–Cl pair; b) Na–O pair; and c) Cl–H pair with the CIP (-----) and the SSIP (——) as an initial structure of AIMD simulations at 100 K. Both the CIP and the SSIP are stable with a sharp RDF peak for Na–Cl (a). The structures are similar to CIP-1 and SSIP shown in Figure 1 with the Na^+ and Cl^- being solvated by 3 water molecules (b and c). The solvent structure of the CIP is less rigid than that of the SSIP, which can be clearly shown by the presence of a third RDF peak of the Cl–H pair for the CIP structure (c).

$\approx$2.8 Å during the entire run (dashed curve) and near 4.6 Å for the SSIP run (solid curve). The Na^+ ion is directly solvated by three water molecules in the first solvation shell ($R_{Na\cdots O}$ = 2.3 Å) and three water molecules in the second solvation shell ($R_{Na\cdots O}$ = 3.7 Å), as indicated by two distinct maxima in the Na···O RDFs (Figure 2b). Finally, three of the water molecules are directly hydrogen-bonded to the Cl^- anion with a Cl···H distance of $\approx$2 Å, as shown in Figure 2c. It is interesting that the solvent structure of the SSIP is more compact with all the other H atoms distributed at the second RDF peak ($R_{Cl\cdots H}$ = 3.6 Å), while a third RDF peak ($R_{Cl\cdots H}$ = 4.8 Å) appears for the CIP structure.

The quantum chemical calculations suggest that entropic effects should favor the CIP configuration, and it is therefore of interest to study the solvation structures of the $NaCl(H_2O)_6$ cluster as a function of temperature. An AIMD simulation was carried out starting from the SSIP configuration at a temperature of $\approx$100 K, and the temperature was then gradually raised to 300 K over a period of 10 ps. The gradual change of temperature (solid line) and the fluctuation of the Na–Cl distance (dashed line) are shown in Figure 3, and a

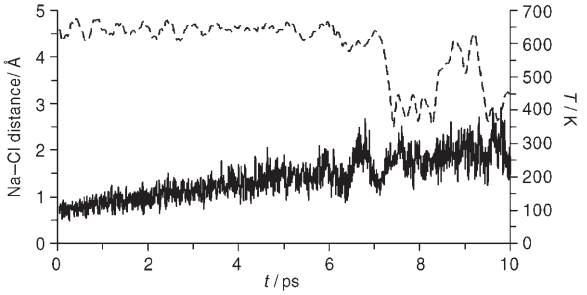

Figure 3. Fluctuation in the distances (-----) of the Na–Cl bond during AIMD simulation on $NaCl(H_2O)_6$ with the temperature (——) raised gradually from 100 to 300 K. The SSIP is unstable at high temperature and eventually converts to the CIP after 7 ps (T>200 K). A movie in mpeg format for the trajectory is available as Supporting Information.

movie of the simulated trajectory is provided in the Supporting Information. In agreement with the ΔG values from quantum chemical calculations, the SSIP configuration becomes unstable and eventually converts to CIP as the temperature increases.

In order to have a clear picture of the instability of the SSIP with increasing temperature, the free energies of the dissolution of Na···Cl in $NaCl(H_2O)_6$ at temperatures of 100 K and 300 K were determined by a series of constrained AIMD simulations, with the Na···Cl distance (R_{Na-Cl}) defined as the reaction coordinate. The R_{Na-Cl} distance was first held fixed at 2.8 Å, the equilibrium distance of Na–Cl in the CIP configuration, and the average force along the Na···Cl bond ($\langle F_{Na-Cl}\rangle$) during a constrained AIMD run was computed. The R_{Na-Cl} distance was then changed from 2.5 Å to 6.0 Å in steps of 0.5 Å. For each constrained R_{Na-Cl} distance, a short AIMD run of 0.5 ps was performed with the temperature of every MD step scaled to the desired value, and then a constant temperature simulation controlled by a Nosé–Hoover thermostat was run with a simulation time of typically 4–8 ps. The simulation was stopped when the standard error of $\langle F_{Na-Cl}\rangle$ was reduced to $\approx 5\,kJ\,mol^{-1}\,Å^{-1}$, as determined by a block averaging method with a correlation time of typically 0.5 ps. The computed $\langle F_{Na-Cl}\rangle$ as a function of the R_{Na-Cl} distance is shown in Figure 4a, where by definition, a negative force corresponds to an attractive interaction.

The reaction free energies ΔG_{Na-Cl} can then be roughly estimated by integration along the curves of $\langle F_{Na-Cl}\rangle$ with respect to R_{Na-Cl}, as shown in Figure 4b:

$$\Delta G_{Na-Cl} = \int -\langle F_{Na-Cl}\rangle dR_{Na-Cl}$$

The ΔG_{Na-Cl} of a configuration at R_{Na-Cl} distance is the free energy of which relative to that of the CIP configuration, the shortest R_{Na-Cl} distance with $\langle F_{Na-Cl}\rangle$ equaling to zero.

Both the CIP and the SSIP structures are apparent at the low temperature of 100 K, with the former being separated by a very small, $\approx 1\,kJ\,mol^{-1}$, energy barrier from the deeper SSIP minimum, some $13\,kJ\,mol^{-1}$ lower in energy than the CIP (solid line in Figure 4b). This situation completely changes at the higher temperature of 300 K, where the CIP structure becomes more stable, with the SSIP minimum disappearing from the free energy profile (dashed line in Figure 4b). Similar temperature-dependence effects were also observed in previous studies on an aqueous NaCl solutions that used the classical molecular dynamics method. These effects were attributed to the decreasing dielectric constant with increasing temperature.[36,39] The effect is believed to be more pronounced in a water cluster than in a bulk aqueous solution because in a finite cluster with only six water molecules, for example, the ionic dissolution of Na···Cl cannot take full advantage of the large solvation entropy available in a bulk aqueous solution.

Conversely, in the SSIP geometry, the water molecules are instrumental in keeping the Na^+ and Cl^- ions apart. In the larger amplitude atomic motions at higher temperatures, the hydrogen bonds between the water molecules and the ions are broken resulting in a collapse of the solvent structure of the SSIP and allowing the Na^+ and Cl^- ions to combine to form the CIP with a less rigid solvent structure. Such dynamic nuclear motion owing to the finite temperature plays a significant role in ionic solvation in small water clusters, and probably also in the solvation chemistry at the air/aerosol interface.[9–12]

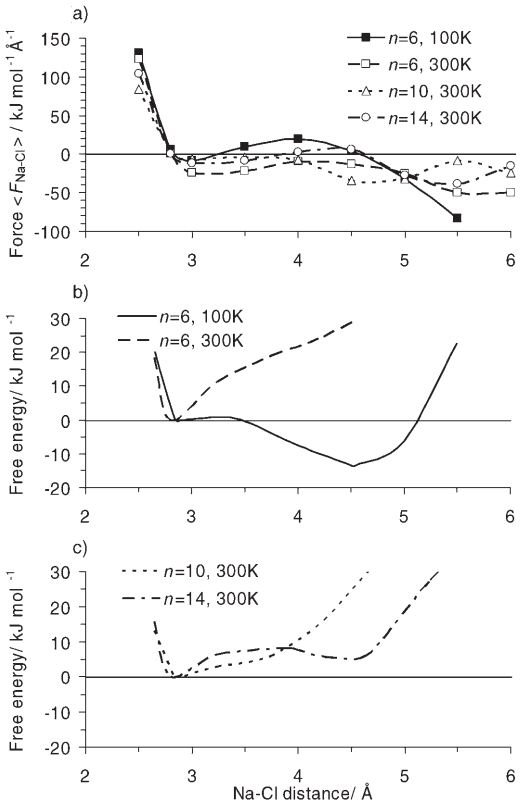

Figure 4. Constrained AIMD simulations at 300 K on $NaCl(H_2O)_n$ with cluster sizes of $n = 6$, 10, and 14 with the Na–Cl distance treated as the reaction coordinate. a) Average forces along the Na–Cl bond $\langle F_{Na-Cl}\rangle$ as a function of the constrained Na–Cl distance R_{Na-Cl}, with negative forces indicating attraction. Integration of $\langle F_{Na-Cl}\rangle$ along the Na–Cl distance gives the free energy for NaCl dissolution: b) $n = 6$ at 100 and 300 K, and c) $n = 10$ and 14 at 300 K.

Ionic dissolution of NaCl in $NaCl(H_2O)_n$, $n = 10$ and 14, at a temperature of 300 K: Similar to the $n = 6$ cluster, the free-energy profiles for the dissolution of NaCl in the larger clusters with $n = 10$ and 14, $NaCl(H_2O)_n$ at a temperature of 300 K were determined by constrained AIMD simulations, as shown in Figure 4c. The equilibrium Na···Cl distance of the CIP configuration, ≈ 2.8 Å according to the current AIMD simulations, is essentially independent of cluster size, and very close to the 2.82 Å determined by X-ray diffraction experiments in a concentrated solution,[19] or to the values determined by theoretical methods that lie between 2.6 and 3.0 Å, depending on the specific method and model potential.[32–34,38,39,58] As expected, the free-energy profiles for $n = 10$ and 14 are significantly changed compared with

the curve for $n = 6$ in Figure 4b. In the $n = 10$ run, the curve (Figure 4c, dotted line) is flattened, with the free energy remaining below 5 kJ mol^{-1} over the Na···Cl distance range between 2.8 and 4.0 Å, and there is just a hint of a second local minimum at a Na···Cl distance of ≈3.8 Å, barely 1 Å longer than in the CIP structure. In the simulation for $n = 14$, the flattened section of the free-energy profile is further broadened, and two distinct minima corresponding to the CIP and SSIP geometries are clearly identifiable.

In the first step of the ionic dissolution of NaCl in a water cluster of $n = 14$, the CIP has to surmount a low barrier of ≈8 kJ mol^{-1} at a Na···Cl distance of 3.9 Å, before it reaches a second, SSIP minimum at a Na···Cl distance of 4.5 Å. This secondary SSIP minimum has a free energy of ≈5 kJ mol^{-1} higher than that of the CIP structure, with the Na···Cl distance of the SSIP structure being already much closer to the bulk aqueous solution value of approximately 5 Å.[32–34,38,39] On the basis of an error of $\langle F_{Na-Cl}\rangle$ (±5 kJ mol^{-1} Å^{-1}) and the incremental value of R_{Na-Cl}, typically 0.5 Å, the uncertainty of the free-energy difference is estimated to be ±3 kJ mol^{-1}, which will not have a qualitative effect on the overall free-energy profile. However, in the relatively flat section of the free-energy surface around the SSIP minimum, the position of the stationary point cannot be determined with a high accuracy.

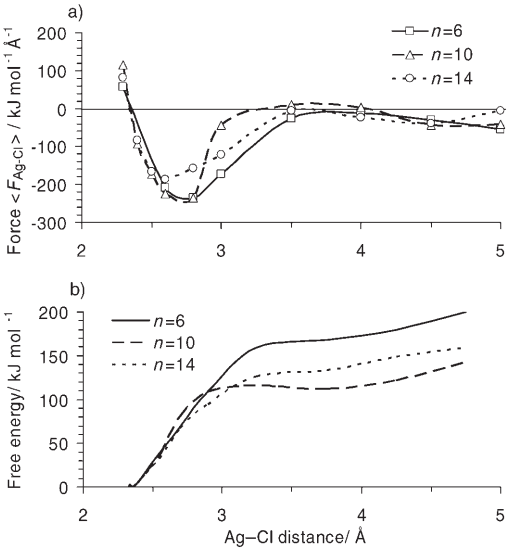

Figure 5. Constrained AIMD simulations at 300 K on AgCl(H$_2$O)$_n$ with cluster sizes of $n = 6$, 10, and 14 with the Ag–Cl distance treated as the reaction coordinate. a) Average forces along the Ag–Cl bond $\langle F_{Ag-Cl}\rangle$ as a function of the constrained Ag–Cl distance R_{Ag-Cl}, with negative force indicating attraction. b) Integration of $\langle F_{Ag-Cl}\rangle$ gives the free energy profile for Ag–Cl dissolution. The attractive force and free energy are both significantly larger than in the case of NaCl in Figure 4.

SSIP and CIP of AgCl(H$_2$O)$_n$ and NaCl(H$_2$O)$_n$ ($n = 6$, 10, and 14) at a temperature of 300 K: To address the central topic of this paper—a comparison between the highly soluble NaCl and AgCl, one of the most insoluble salts—we have now similarly examined the dissolution of AgCl. The main results are summarized in Figure 5. As in the case of NaCl, the free-energy profiles for the ionic dissolution of AgCl in AgCl(H$_2$O)$_n$ clusters with sizes of $n = 6$, 10, and 14, were again explored by constrained AIMD simulations at a temperature of 300 K, with average force errors $\langle F_{Ag-Cl}\rangle$ of ≈10 kJ mol^{-1} Å^{-1} along the Ag···Cl bond. Figure 5a shows the $\langle F_{Ag-Cl}\rangle$, with the CIP with zero force at a distance of ≈2.35 Å, fairly close to the gas-phase Ag–Cl bond length of 2.281 Å.[80] It is interesting to compare this with the result of sodium chloride, where the CIP configuration Na–Cl distance in NaCl(H$_2$O)$_n$ clusters, approximately 2.8 Å, is significantly longer than the gas-phase value of the Na–Cl bond length, 2.361 Å.[81] Clearly, the more covalent AgCl is less strongly affected by the water molecules than the more polar NaCl.

In agreement with the macroscopic solvation behavior—the solubility of AgCl is roughly 10^{11} times lower than that of NaCl—the attractive forces between Ag$^+$ and Cl$^-$ in the AgCl(H$_2$O)$_n$ clusters (Figure 5a) are much stronger than those between Na$^+$ and Cl$^-$ in NaCl(H$_2$O)$_n$. The dominant factor governing the solubility difference between NaCl and AgCl in aqueous solution is the ionic dissociation energy of the Na–Cl and the Ag–Cl bonds, as can easily be shown using appropriate Born–Haber cycles for their dissolution processes.[45] From Figure 5b, it is evident that, in the first step of the ionic dissolution of AgCl, the separation of the Ag$^+$ and Cl$^-$ ions would have to overcome a significant barrier in the 2.3 to 3.5 Å separation range. The interionic attraction of AgCl in this region is much stronger than that of NaCl, which leads to a steep increase in the free energy for the dissolution of AgCl to more than 100 kJ mol^{-1} (Figure 5b), compared with only 10 kJ mol^{-1} for NaCl (Figure 4c). In agreement with very recent DFT studies,[60] the AgCl CIP is much more stable than AgCl SSIP in water clusters, and the dynamics of nuclear motions included in our work further destabilize the AgCl SSIP configuration. Beyond the 3.5 Å interionic distance, the forces along the dissolution coordinate for both NaCl(H$_2$O)$_n$ and AgCl(H$_2$O)$_n$ are more comparable.

From first-year chemistry, we know that the highly soluble NaCl is easily ionized in aqueous solutions, with the Na$^+$ and Cl$^-$ ions well solvated and stabilized by the solvent molecules. Our calculations also show that the dissolution of a CIP to form a SSIP requires much less energy for NaCl than for AgCl in water clusters. In order to explore in more detail such solubility difference of NaCl and AgCl in water clusters, the stability of the SSIP configuration in NaCl(H$_2$O)$_n$ and AgCl(H$_2$O)$_n$ were examined for cluster sizes of $n = 6$, 10, and 14 at a temperature of 300 K by means of the constraint-free AIMD method. For NaCl(H$_2$O)$_n$, each of the AIMD simulations was started from the SSIP initial configuration, with the Na···Cl distance longer than 4.5 Å, and the cluster was thermally equilibrated in 500 steps before the Nosé–Hoover thermostat was activated. The simulation then ran for 5 ps. The stability of the SSIP can then be monitored by following the fluctuations of the Na···Cl dis-

tance along the AIMD trajectories, as shown in Figure 6a. As expected from the calculated free-energy profile of the ionic dissolution of NaCl in $NaCl(H_2O)_6$ (dashed line in Figure 4b), the SSIP structure of $n = 6$ is not stable and "precipitates" during the simulation rapidly to form the CIP at an Na···Cl distance of ≈2.8 Å (solid curve in Figure 6a), the reverse process of the ionic dissolution studied by the above constrained dynamics simulations. The SSIP structure of $n = 10$ is relatively stable; however, the geometry intermittently changes to CIP. Finally, in the $n = 14$ simulation, the SSIP structure remains stable over the entire 5 ps of the simulation.

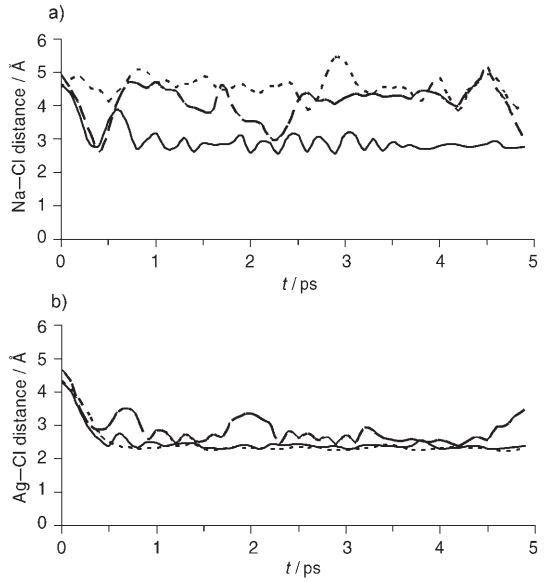

Figure 6. Fluctuation of the interionic distance during AIMD simulations at 300 K. a) On $NaCl(H_2O)_n$ with $n = 6$ (——), 10 (-----), and 14 (•••••), starting from an initial geometry with a Na–Cl distance longer than 4.5 Å. b) On $AgCl(H_2O)_n$ with $n = 6$ (——), 10 (-----), and 14 (•••••), starting from an initial geometry with an Ag–Cl distance longer than 4.0 Å. For $NaCl(H_2O)_n$, the stability of the SSIP configuration increases with increasing cluster size. For $AgCl(H_2O)_n$, "precipitation" immediately takes place for all the cluster sizes studied. Movies in mpeg format for the trajectories of both $NaCl(H_2O)_{14}$ and $AgCl(H_2O)_{14}$ clusters are provided as Supporting Information.

Similar to $NaCl(H_2O)_n$, we have also performed constraint-free AIMD simulations for $AgCl(H_2O)_n$ clusters with sizes of $n = 6$, 10, and 14. Starting from a SSIP initial structure and an Ag···Cl distance of 4.5 Å, the cluster was thermally equilibrated in 500 steps before the Nosé–Hoover thermostat was activated. Actually, as discussed before, the SSIP configuration for $AgCl(H_2O)_n$ does not really exist in the finite clusters as a local minimum on the free energy profile. However, for the convenience of the present discussion, we will still refer to Ag^+/Cl^- as SSIP when the Ag–Cl separation is greater than ≈3.5 Å, where the free energy profile reaches a plateau. As expected, the SSIP configuration is unstable, and a rapid "precipitation" takes place during the AIMD run for all sizes studied to yield the CIP configuration, as clearly shown in Figure 6b. The rapid precipitation of the SSIP of $AgCl(H_2O)_{14}$, comparing with the stable SSIP of $NaCl(H_2O)_{14}$, in the 5 ps AIMD simulation at 300 K can also be seen in the movies of the trajectories, available as Supporting Information.

Solvation structures of $NaCl(H_2O)_n$ and $AgCl(H_2O)_n$: The dissolution of the NaCl and AgCl molecules and the solvation energies are also strongly affected by differences in the CIP and SSIP geometries in the $NaCl(H_2O)_n$ and $AgCl(H_2O)_n$ clusters. One useful way to describe a solvated ion or molecule is to use the coordination number, which is the number of solvent molecules in the first solvation shell that are in direct contact with the ions. Obviously, in a fluxional water cluster assigning the solvent molecules to the first solvation shell is somewhat arbitrary; however, for the purpose of the present discussion we consider a water molecule to be in the first solvation shell if its distance from the corresponding ion is less than the minimum beyond the first peak on the respective radial distribution function (RDF).

The RDFs for Na···O, Ag···O, and Cl···H pairs of the CIP configurations in clusters $n = 6$, 10, and 14, obtained from the above constrained AIMD simulations (Na–Cl = 2.8 Å and Ag–Cl = 2.35 Å), are shown in Figure 7. The coordination number of Na in the CIP for all studied cluster sizes is about 3, which can be seen by integrating the first peak of the Na···O RDF curve (≈2.3 Å, Figure 7a). Interestingly,

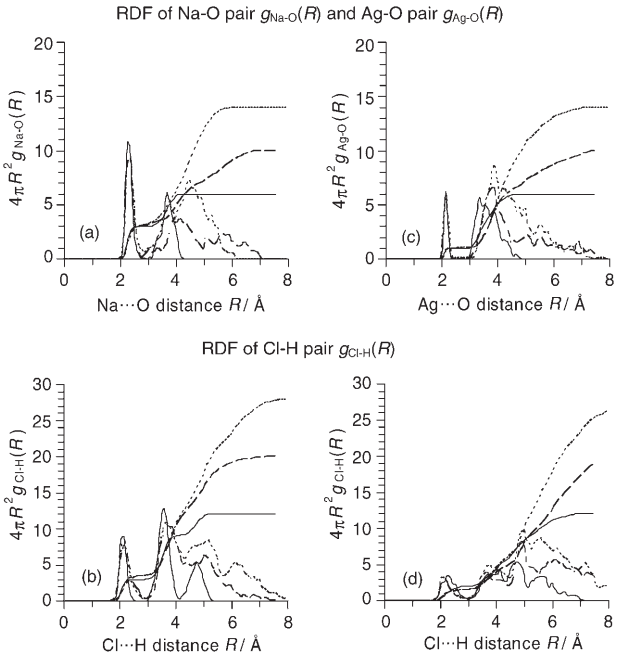

Figure 7. Radial distribution functions (RDF) of CIP structures with $n = 6$ (——), 10 (-----), and 14 (•••••), and curves of their integration, of a) Na-O and b) Cl-H for $NaCl(H_2O)_n$; of c) Ag-O and d) Cl-H pairs for $AgCl(H_2O)_n$; taken from constrained AIMD simulations at 300 K (Figures 5 and 6). The coordination number (CN) of Na (≈3) is higher than that of Ag (≈1) and the CN of Cl in $NaCl(H_2O)_n$ (≈3) is also higher than that in $AgCl(H_2O)_n$ (≈2), which indicates that the water molecules interact more strongly with NaCl CIP than with AgCl CIP.

the coordination number of Ag obtained by integrating the first peak of the Ag···O RDF (≈2.2 Å, Figure 7c) is only one, reflecting the formation of a quasilinear, hydrated H_2O-Ag-Cl complex. From the first RDF peak of Cl···H (≈2.1 Å, Figure 7b and d), the coordination number of Cl for NaCl is ≈3, which is also higher than the value of ≈2 for AgCl. The higher coordination number of NaCl is again in agreement with the fact that NaCl interacts more strongly with water molecules.

Intuitively, one must expect the coordination number to change during the dissolution process. The initial coordination number depends on the structure of the CIP, and as the distance between the ions increases, additional water molecules penetrate the area between them, and may enter the first solvation shell, increasing the coordination number. The mean coordination numbers during the constrained dynamic runs and their change along the reaction coordinate as the interionic distance is increased are shown for NaCl and AgCl in the $n = 6$, 10 and 14 clusters in Figure 8. For

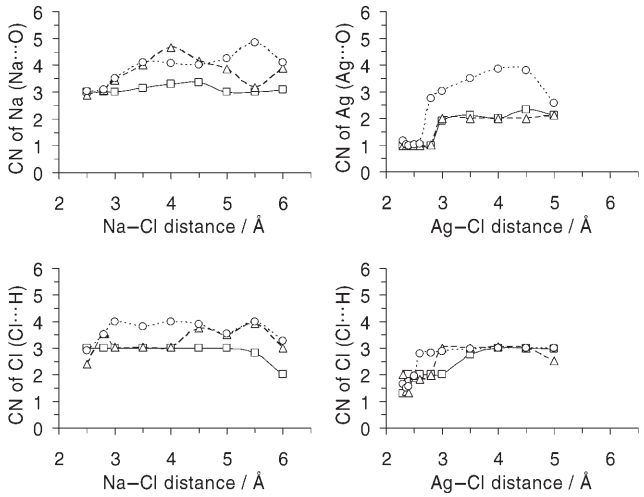

Figure 8. Mean coordination numbers during the constrained AIMD simulations for $NaCl(H_2O)_n$ and $AgCl(H_2O)_n$ for $n = 6$ (□), 10 (△), and 14 (○), and their change along the reaction coordinate as the interionic distance is increased. The coordination numbers of NaCl are generally higher than those of AgCl.

most cluster sizes, the coordination number initially increases as the salt molecule dissociates and the distance between the ions grows. The decrease, which most curves show near the maximum distance, is easily understandable: the ions must eventually approach the surface of the finite clusters.

For $NaCl(H_2O)_n$, the coordination number of Na^+ starts close to three for the CIP configuration, at a Na···Cl distance of 2.8 Å, and it gradually increases to about four at a Na···Cl distance above 4.5 Å. For $AgCl(H_2O)_n$, in spite of the higher solvation energy of Ag^+ compared with Na^+,[82] the coordination number of Ag^+ starts close to one for the CIP configuration, at a Ag···Cl distance of 2.35 Å, and it increases for both the $n = 6$ and 10 clusters to about two at longer interionic separations. Only for the largest cluster studied, $n = 14$, the coordination number gradually increases to nearly four at large separations. This behavior reflects the delicate interplay between the propensity of Ag^+ to undergo two-fold linear coordination, and the necessity to integrate such a complex into a hydrogen-bonded network.[83] Such two-fold linear coordination of Ag^+, H_2O-Ag-Cl, which is attributed to sd hybridization of Ag^+,[83,84] is further characterized by the orientation of the water ligands in the first shell of Ag^+ (Figure S1 in the Supporting Information). The sd_{z^2}-hybridized orbital generates a hole of reduced electronic charge along the z axis.[83,84] A lone pair of a water molecule interacts with that hole and another lone pair of the water molecule can form hydrogen bond to the water cluster. For Na^+, the cationic charge is spherically distributed, so that both lone pairs of a water molecule can interact with the Na^+, so that Na^+ may have a higher coordination number than Ag^+.

Figures 9 (NaCl) and 10 (AgCl) show typical geometries that have been taken from a snapshot near the end of the constrained AIMD run at the respective distance. The NaCl CIP is internally solvated by the water cluster for all cluster sizes. On the other hand, the AgCl CIP is weakly solvated at the surface of the water clusters. Similar surface-solvated structures were suggested for $NaI(H_2O)_n$ clusters with the NaI CIP being dominant even in a large cluster size of 50 water molecules.[42] While the Na^+/Cl^- SSIP structures

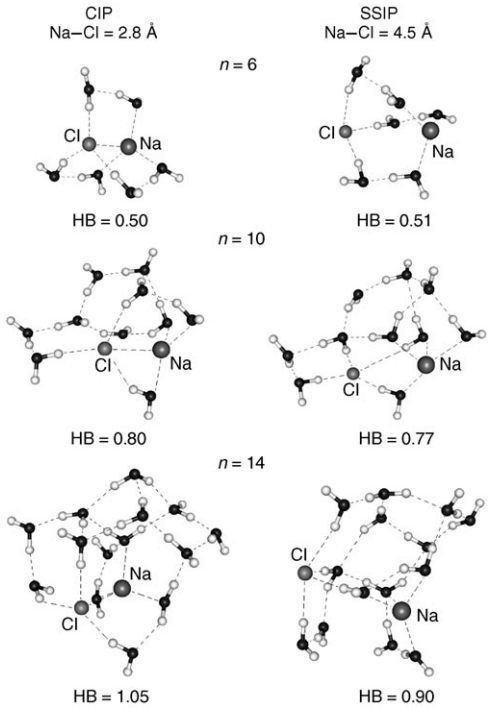

Figure 9. Structures of $NaCl(H_2O)_n$, $n = 6$, 10 and 14, with the Na–Cl distance fixed at 2.8 Å and 4.5 Å. The structures are taken from a snapshot near the end of the constrained AIMD run at the respective distance. NaCl is internally solvated for both the CIP and the SSIP configurations. The number of hydrogen bonds (H···O) per water molecule (HB) is the average obtained from the AIMD run, where a hydrogen bond is counted when O···H lies between 1.2 Å and 2.0 Å.

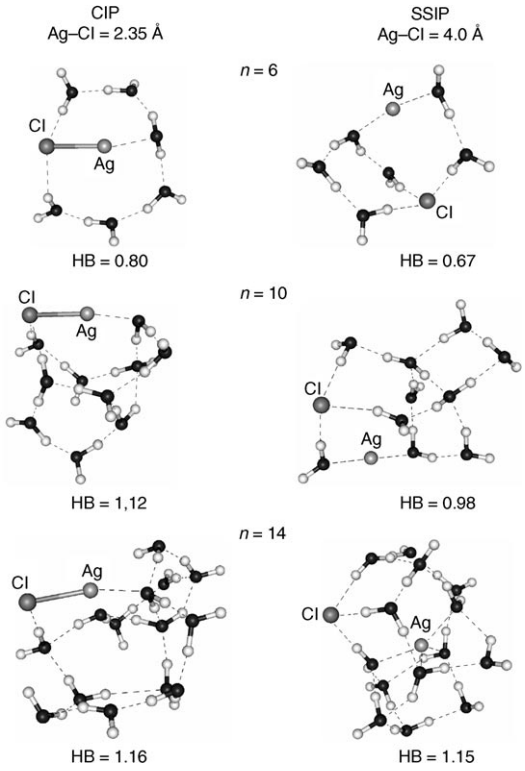

Figure 10. Structures of $AgCl(H_2O)_n$, $n = 6$, 10 and 14, with the Ag–Cl distance fixed at 2.35 and 4.0 Å. The structures are taken from a snapshot near the end of the constrained AIMD run at the respective distance. AgCl is solvated at the surface for the CIP configuration and reluctantly changes to internal solvation for the SSIP configuration. The number of hydrogen bonds (H···O) per water molecule (HB) is the average obtained from the AIMD run, where a hydrogen bond is counted when O···H lies between 1.2 and 2.0 Å.

are again internally solvated, the Ag^+/Cl^- SSIP structures for $n = 6$ and 10 are still weakly solvated on the cluster surface, and an internally solvated structure reluctantly forms only for the $n = 14$ cluster.

The AgCl CIP is weakly solvated at the surface of a water cluster, while the NaCl CIP is internally solvated, probably because the less polar AgCl (6.07 D) is less hydrophilic than the more polar NaCl (8.97 D). In addition, the more polarizable AgCl probably has a higher propensity than the less polarizable NaCl to stay on the surface of a water cluster, a similar effect to the previously described enrichment of halide ions on the surface of water droplets.[85–87] This is in agreement with the estimated average number of hydrogen bonds H···O per water molecule (HB), where a hydrogen bond is counted when an O···H distance $R_{O\cdots H}$ is $1.2 < R_{O\cdots H} < 2.0$ Å. In all cases, the HB of $AgCl(H_2O)_n$ is larger than that of the corresponding $NaCl(H_2O)_n$, both for the CIP and the SSIP structure. It seems that AgCl has a reduced hydrophilicity, although it is not hydrophobic, so that water molecules prefer to interact with each other and do not solvate AgCl efficiently. This may accelerate precipitation reactions in the bulk and lead to the rapid precipitation of AgCl in aqueous solutions.

The major difference between NaCl and AgCl in their solvation structure is that NaCl is always well solvated inside the water clusters, while the dissolution of AgCl requires a significant reorganization of the solvent structure in order to convert the surface-solvated CIP configuration to an internally solvated SSIP. This solvent reorganization is a complex process, which is of fundamental importance for a microscopic understanding of ion solvation.

Summary

The free energy of ionic dissolution of NaCl and AgCl in $NaCl(H_2O)_n$ and $AgCl(H_2O)_n$, respectively, and their solvation structures at cluster sizes of $n = 6$, 10, and 14, have been studied by AIMD simulations. A detailed study of $NaCl(H_2O)_n$ revealed that the minimum cluster size needed to stabilize both the CIP and SSIP configurations are temperature-dependent. Both the CIP and the SSIP of $NaCl(H_2O)_6$ are apparent at a low temperature of 100 K, while the SSIP is unstable at a high temperature of 300 K. At the higher temperature, the hydrogen bonds rearrange more readily so that the more rigid solvent structure of the SSIP can collapse and allow the Na^+ and Cl^- ions to combine and form the CIP with a less rigid solvent structure. Chemical intuition attributes higher entropy to the SSIP than to the CIP structure. The calculations, however, show that a highly ordered arrangement of water molecules is necessary in gas-phase clusters to stabilize the SSIP, which actually leads to a lower entropy than that of the CIP structure. Similar arguments may apply to highly concentrated or saturated salt solutions.

The Na–Cl distance of 2.8 Å for the CIP configuration is nearly independent of the cluster size. In agreement with the high solubility in bulk solution, the SSIP becomes more stable with increasing cluster size, as indicated by the clearly identifiable local minima on the free-energy surface at Na–Cl distances of 3.8 and 4.5 Å for $n = 10$ and 14, respectively.

The interionic attraction of AgCl is much stronger than that of NaCl for all cluster sizes studied, and the free energy for the ionic dissolution of AgCl rises steeply to more than 100 kJ mol^{-1}, compared to only 10 kJ mol^{-1} for NaCl. The large difference in ionic dissociation energies results in an equally large difference in solvation structures between $NaCl(H_2O)_n$ and $AgCl(H_2O)_n$. NaCl is strongly internally solvated by the water cluster both for the CIP and SSIP configurations, while the AgCl CIP is solvated at the surface of the water clusters because of the weaker AgCl–water interaction. The ionic dissolution of AgCl therefore requires a significant rearrangement of the solvent structure in $AgCl(H_2O)_n$. The less hydrophilic properties of AgCl may contribute to the rapid precipitation of AgCl from aqueous solutions.

Acknowledgements

We thank the Leibniz Computing Center in Munich for allocating computer time. Financial support of the Alexander von Humboldt Foundation (C.K.S.) and the Fonds der Chemischen Industrie is gratefully acknowledged.

[1] B. E. Conway, *Ionic Hydration in Chemistry and Biophysics*, Elsevier Scientific Publishing Company, Amsterdam, **1981**.
[2] Y. Marcus, *Ion Solvation*, Wiley, New York, **1985**.
[3] M. P. Apse, G. S. Aharon, W. A. Snedden, E. Blumwald, *Science* **1999**, *285*, 1256–1258.
[4] T. Cserháti, E. Forgács, *Int. J. Pharm.* **2003**, *254*, 189–196.
[5] P. Neysens, W. Messens, L. De Vuyst, *Int. J. Food Microbiol.* **2003**, *88*, 29–39.
[6] P. Rodríguez, A. Torrecillas, M. A. Morales, M. F. Ortuño, M. J. Sánchez-Blanco, *Environ. Exp. Bot.* **2005**, *53*, 113–123.
[7] W. B. Jakoby, *Crystallization as a purification technique, Enzyme Purification and Related Techniques, in Methods in Enzymology, Vol. 22*, Academic Press, New York, **1971**.
[8] B. N. Asmar, P. Ergenzinger, *Hydrocarbon Process.* **2002**, *16*, 2819–2831.
[9] E. E. Gard, M. J. Kleeman, D. S. Gross, L. S. Hughes, J. O. Allen, B. D. Morrical, D. P. Fergenson, T. Dienes, M. E. Gälli, R. J. Johnson, G. R. Cass, K. A. Prather, *Science* **1998**, *279*, 1184–1187.
[10] K. W. Oum, M. J. Lakin, D. O. DeHaan, T. Brauers, B. J. Finlayson-Pitts, *Science* **1998**, *279*, 74–77.
[11] E. M. Knipping, M. J. Lakin, K. L. Foster, P. Jungwirth, D. J. Tobias, R. B. Gerber, D. Dabdub, B. J. Finlayson-Pitts, *Science* **2000**, *288*, 301–306.
[12] B. J. Finlayson-Pitts, *Chem. Rev.* **2003**, *103*, 4801–4822.
[13] L. E. de-Bashan, Y. Bashan, *Water Res.* **2004**, *38*, 4222–4246.
[14] N. Tsipouras, C. J. Rix, P. H. Brady, *Clin. Chem.* **1997**, *43*, 290–301.
[15] S. Balasch, R. Romero, A. Ferrer, *Nat. Hazards* **2004**, *32*, 345–355.
[16] K. Ichikawa, Y. Kameda, T. Matsumoto, M. Misawa, *J. Phys. C* **1984**, *17*, L725–L729.
[17] A. G. Miller, J. W. Macklin, *J. Phys. Chem.* **1985**, *89*, 1190–1193.
[18] J. E. Enderby, S. Cummings, G. J. Herdman, G. W. Neilson, P. S. Salmon, N. Skipper, *J. Phys. Chem.* **1987**, *91*, 5851–5858.
[19] H. Ohtaki, N. Fukushima, *J. Solution Chem.* **1992**, *21*, 23–38.
[20] W. Rudolph, M. H. Brooker, C. C. Pye, *J. Phys. Chem.* **1995**, *99*, 3793–3797.
[21] Y. Kameda, M. Imano, M. Takeuchi, S. Suzuki, T. Usuki, O. Uemura, *J. Non-Cryst. Solids* **2001**, *293–295*, 600–606.
[22] Y. Kameda, N. Kudoh, S. Suzuki, T. Usuki, O. Uemura, *Bull. Chem. Soc. Jpn.* **2001**, *74*, 1009–1014.
[23] M. Alves Marques, M. I. Cabaço, M. I. de Barros Marques, A. M. Gaspar, *J. Phys. Condens. Matter* **2002**, *14*, 7427–7448.
[24] T. Megyes, T. Radnai, A. Wakisaka, *J. Phys. Chem. A* **2002**, *106*, 8059–8065.
[25] E. V. Vinogradov, P. R. Smirnov, V. N. Trostin, *Russ. Chem. Bull.* **2003**, *52*, 1253–1271.
[26] A. M. Gaspar, M. Alves Marques, M. I. Cabaço, M. I. de Barros Marques, T. Buslaps, V. Honkimaki, *J. Mol. Liq.* **2004**, *110*, 15–22.
[27] M. Alves Marques, M. I. de Barros Marques. , M. I. Cabaço, A. M. Gaspar, M. L. de Almeida, *J. Mol. Liq.* **2004**, *110*, 23–31.
[28] A. C. Belch, M. Berkowitz, J. A. McCammon, *J. Am. Chem. Soc.* **1986**, *108*, 1755–1761.
[29] G. Heinje, W. A. P. Luck, K. Heinzinger, *J. Phys. Chem.* **1987**, *91*, 331–338.
[30] E. Guàrdia, J. A. Padró, *J. Phys. Chem.* **1990**, *94*, 6049–6055.
[31] E. Guàrdia, R. Rey, J. A. Padró, *J. Chem. Phys.* **1991**, *95*, 2823–2831.
[32] R. Rey, J. A. Padró, *J. Phys. Chem.* **1992**, *96*, 4712–4718.
[33] S.-B. Zhu, G. W. Robinson, *J. Chem. Phys.* **1992**, *97*, 4336–4348.
[34] D. E. Smith, L. X. Dang, *J. Chem. Phys.* **1994**, *100*, 3757–3766.
[35] A. A. Chialvo, P. T. Cummings, H. D. Cochram, J. M. Simonson, R. E. Mesmer, *J. Chem. Phys.* **1995**, *103*, 9379–9387.
[36] A. A. Chialvo, P. T. Cummings, J. M. Simonson, R. E. Mesmer, *J. Chem. Phys.* **1996**, *105*, 9248–9257.
[37] S. Izvekov, M. R. Philpott, *J. Chem. Phys.* **2000**, *113*, 10676–10684.
[38] J. Martí, F. S. Csajka, *J. Chem. Phys.* **2000**, *113*, 1154–1161.
[39] A. Y. Zasetsky, I. M. Svishchev, *J. Chem. Phys.* **2001**, *115*, 1448–1454.
[40] Z.-G. Zhang, Z.-H. Duan, *Chem. Phys.* **2004**, *297*, 221–233.
[41] Y. Gauduel, H. Gelabert, M. Ashokkumar, *Chem. Phys.* **1995**, *197*, 167–193.
[42] G. Grégoire, M. Mons, C. Dedonder-Lardeux, C. Jouvet, *Eur. Phys. J. D* **1998**, *1*, 5–7.
[43] C. Dedonder-Lardeux, G. Grégoire, C. Jouvet, S. Martrenchard, D. Solgadi, *Chem. Rev.* **2000**, *100*, 4023–4037.
[44] G. Grégoire, M. Mons, I. Dimicoli, C. Dedonder-Lardeux, C. Jouvet, S. Martrenchard, D. Solgadi, *J. Chem. Phys.* **2000**, *112*, 8794–8805.
[45] B. Fox, M. K. Beyer, U. Achatz, S. Joos, G. Niedner-Schatteburg, V. E. Bondybey, *J. Phys. Chem. A* **2000**, *104*, 1147–1151.
[46] V. E. Bondybey, M. K. Beyer, *Int. Rev. Phys. Chem.* **2002**, *21*, 277–306.
[47] S. M. Hurley, T. E. Dermota, D. P. Hydutsky, A. W. Castleman, *Science* **2002**, *298*, 202–204.
[48] A. J. Huneycutt, R. J. Saykally, *Science* **2003**, *299*, 1329–1330.
[49] T. Schindler, C. Berg, G. Niedner-Schatteburg, V. E. Bondybey, *Chem. Phys. Lett.* **1994**, *229*, 57–64.
[50] G. Niedner-Schatteburg, V. E. Bondybey, *Chem. Rev.* **2000**, *100*, 4059–4086.
[51] *Handbook of Chemistry and Physics*, CRC Press, Boca Raton, **1996**.
[52] G. Makov, A. Nitzan, *J. Phys. Chem.* **1992**, *96*, 2965–2967.
[53] T. Asada, K. Nishimoto, *Chem. Phys. Lett.* **1995**, *232*, 518–523.
[54] D. E. Woon, T. H. Dunning Jr., *J. Am. Chem. Soc.* **1995**, *117*, 1090–1097.
[55] C. P. Petersen, M. S. Gordon, *J. Phys. Chem. A* **1999**, *103*, 4162–4166.
[56] P. Jungwirth, *J. Phys. Chem. A* **2000**, *104*, 145–148.
[57] A. Mizoguchi, Y. Ohshima, Y. Endo, *J. Am. Chem. Soc.* **2003**, *125*, 1716–1717.
[58] Z. S. Zidi, *J. Chem. Phys.* **2005**, *123*, 064309.
[59] B. S. Fox, O. P. Balaj, I. Balteanu, M. K. Beyer, V. E. Bondybey, *J. Am. Chem. Soc.* **2002**, *124*, 172–173.
[60] S. S. M. C. Godinho, P. C. do Couto, B. J. C. Cabral, *J. Chem. Phys.* **2005**, *122*, 044316.
[61] A. A. Migdisov, A. E. Williams-Jones, O. M. Suleimenov, *Geochim. Cosmochim. Acta* **1999**, *63*, 3817–3827.
[62] F. Bournel, C. Mangeney, M. Tronc, *Phys. Rev. B* **2002**, *65*, 201404.
[63] S. C. Park, H. Kang, *J. Phys. Chem. B* **2005**, *109*, 5124–5132.
[64] M. C. Payne, M. P. Teter, D. C. Allan, T. A. Arias, J. D. Joannopoulos, *Rev. Mod. Phys.* **1992**, *64*, 1045–1097.
[65] D. Marx, J. Hutter in *Modern Methods and Algorithms of Quantum Chemistry, Vol. 1* (Ed.: J. Grotendorst), John von Neumann Institute for Computing, Jülich, **2000**, pp. 301–449.
[66] J. S. Tse, *Annu. Rev. Phys. Chem.* **2002**, *53*, 249–290.
[67] G. Kresse, J. Hafner, *Phys. Rev. B* **1993**, *47*, 558–561.
[68] G. Kresse, J. Hafner, *Phys. Rev. B* **1994**, *49*, 14251–14269.
[69] G. Kresse, J. Furthmuller, *Phys. Rev. B* **1996**, *54*, 11169–11186.
[70] G. Kresse, J. Furthmuller, *Comput. Mater. Sci.* **1996**, *6*, 15–50.
[71] J. P. Perdew, Y. Wang, *Phys. Rev. B* **1992**, *45*, 13244–13249.
[72] G. Kresse, D. Joubert, *Phys. Rev. B* **1999**, *59*, 1758–1775.
[73] P. E. Blöchl, *Phys. Rev. B* **1994**, *50*, 17953–17979.
[74] Gaussian 98, Revision A11, M. J. Frisch, G. W. Trucks, H. B. Schlegel, G. E. Scuseria, M. A. Robb, J. R. Cheeseman, V. G. Zakrzewski, J. A. Montgomery Jr., R. E. Stratmann, J. C. Burant, S. Dapprich, J. M. Millam, A. D. Daniels, K. N. Kudin, M. C. Strain, O. Farkas, J. Tomasi, V. Barone, M. Cossi, R. Cammi, B. Mennucci, C. Pomelli, C. Adamo, S. Clifford, J. Ochterski, G. A. Petersson, P. Y. Ayala, Q. Cui, K. Morokuma, D. K. Malick, A. D. Rabuck, K. Raghavachari, J. B. Foresman, J. Cioslowski, J. V. Ortiz, A. G. Baboul, B. B. Stefanov, G. Liu, A. Liashenko, P. Piskorz, I. Komaromi, R. Gomperts, R. L. Martin, D. J. Fox, T. Keith, M. A. Al-Laham, C. Y. Peng, A. Nanayakkara, C. Gonzalez, M. Challacombe, P. M. W. Gill, B. John-

son, W. Chen, M. W. Wong, J. L. Andres, C. Gonzalez, M. Head-Gordon, E. S. Replogle, J. A. Pople, Gaussian Inc., Pittsburgh PA, **1998**.
[75] I. Dzidic, P. Kebarle, *J. Phys. Chem.* **1970**, *74*, 1466–1474.
[76] P. M. Holland, A. W. Castleman Jr., *J. Chem. Phys.* **1982**, *76*, 4195–4205.
[77] R. G. Keesee, A. W. Castleman Jr., *Chem. Phys. Lett.* **1980**, *74*, 139–142.
[78] S. Nosé, *J. Chem. Phys.* **1984**, *81*, 511–519.
[79] H. C. Anderson, *J. Comp. Physiol.* **1983**, *52*, 24–34.
[80] E. Pearson, W. Gordy, *Phys. Rev.* **1966**, *152*, 42.
[81] Z. K. Ismail, R. H. Hauge, J. L. Margrave, *J. Mol. Spectrosc.* **1975**, *54*, 402–411.
[82] P. W. Atkins, *Physical Chemistry*, Oxford University Press, New York, **1998**.
[83] B. S. Fox, M. K. Beyer, V. E. Bondybey, *J. Am. Chem. Soc.* **2002**, *124*, 13613–13623.
[84] L. E. Orgel, *J. Chem. Soc.* **1958**, *90*, 4186–4190.
[85] P. Jungwirth, D. J. Tobias, *J. Phys. Chem. B* **2001**, *105*, 10468–10472.
[86] P. Jungwirth, D. J. Tobias, *J. Phys. Chem. B* **2002**, *106*, 6361–6373.
[87] S. Ghosal, J. C. Hemminger, H. Bluhm, B. S. Mun, E. L. D. Hebenstreit, G. Ketteler, D. F. Ogletree, F. G. Requejo, M. Salmeron, *Science* **2005**, *307*, 563–566.

Received: December 14, 2005
Revised: February 8, 2006
Published online: May 23, 2006

